Available online at www.sciencedirect.com
ScienceDirect
Journal of Crystal Growth 304 (2007) 497–503
JOURNAL OF CRYSTAL GROWTH
www.elsevier.com/locate/jcrysgro

Model study of local enhancement of chemical potential gradient after facet formation on growing spherical $Cu_{2-\delta}Se$ crystals

Davorin Lovrić*, Zlatko Vučić, Jadranko Gladić

Institute of Physics, Bijenička cesta 46, P.O. Box 304, 10000 Zagreb, Croatia

Received 9 August 2006; received in revised form 23 January 2007; accepted 27 February 2007
Communicated by Y. Furukawa
Available online 12 March 2007

Abstract

The growth of spherical copper selenide single crystals (fed by Cu atoms at constant rate) is driven by the gradient of the chemical potential, which is in the absence of facets isotropic and proportional to inverse square of crystal radius. We investigate the influence of the facets on the local chemical potential gradient on the facet site by a model based on diffusion of Cu atoms with appropriate boundary conditions. The average chemical potential gradient decreases as crystal grows, acquiring values that are, except for the initial growing period, below the threshold value for activation of 2D nucleation. We show that in spite of this fact the local chemical potential gradient, due to the facet presence, may acquire large values, sufficient to activate 2D nucleation and to justify the occurrence of the growing mode consisting of alternation of time intervals of facet vertical growth with those in which facet does not advance, as has been preliminary detected in our experiments.

PACS: 81.10.−h; 81.10.Aj

Keywords: A1. Growth models; A1. Nucleation; A1. Supersaturation; A2. Single crystal growth; B2. Superionic conductors

1. Introduction

The growth of ^{4}He single crystals at temperatures ranging from 2 to 250 mK, under the conditions of constant influx of He atoms, at average growth rates higher than 1 nm/s reveals new growth mode of the *c*-facet in the direction perpendicular to the facet, named burst-like growth mode [1,2]. This peculiar growth is characterized by almost regular alternation of intervals of fast facet vertical growth with the intervals during which the facet does not grow. As the growth temperature increases, the values of threshold pressures at which the penetration of the barrier for facet growth occurs become higher, but more spread as well. Because of this unexpected temperature dependence of the average threshold pressure for nucleation, an interpretation based on the quantum tunnelling has been suggested [2].

We have investigated the growth of the superionic conductor copper selenide at temperatures somewhat beneath the roughening temperature, i.e. at about 800 K [3]. This material belongs to the class of mixed conductors with high both ionic and electronic conductivity (being about 10^2 and 10^5 S/m, respectively) in a wide temperature range (300–1400 K) [4], and as such is a material with very high bulk diffusivity of copper atoms upon which the fast crystal shape relaxation is based.

The growth has been performed under the conditions (described in quite some details in Ref. [3]) of constant material influx, controlled by a constant chemical potential difference and a chosen suitable geometry of the capillary (Fig. 1) in order to ensure Cu atom flux controlled growth mode, $j_{Cu}/j_{Se} < 10^{-5}$ [3].

The source of Cu atoms has been a piece of metallic copper, which fixes the upper value of chemical potential. The chemical potential at the opposite end, i.e. on the surface of the growing spherical crystal, has been fixed by the vapour pressure of the surrounding Se, which is in fact

*Corresponding author. Tel.: +385 1 4698864; fax: +385 1 4698889.
E-mail address: lovric@ifs.hr (D. Lovrić).

0022-0248/$ - see front matter © 2007 Elsevier B.V. All rights reserved.
doi:10.1016/j.jcrysgro.2007.02.028

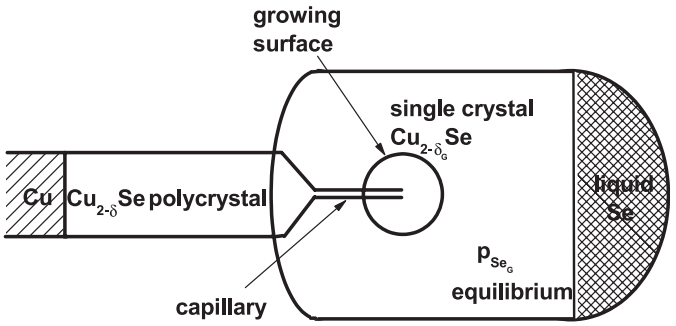

Fig. 1. Schematics of the geometry of growth of copper selenide single crystals.

the equilibrium vapour pressure of the particular chosen stoichiometry of the growing crystal. Between these two extreme points of chemical potential, a continuous distribution of copper atoms' density develops, from Cu_2Se at the contact with metallic copper to, say, $Cu_{1.8}Se$ at the very surface of the growing crystal. This copper ion density follows the specific geometry along the path of transport of Cu atoms (cf. Fig. 5 of Ref. [3]). We note that the dominant drop (more than 99%) of the chemical potential occurs at the capillary orifice. As a result, due to the constant (better than 1%) copper atom flux through the capillary orifice, a spherical single crystal has grown on top of the capillary tip, having a volume which has been shown to increase linearly in time for more than five decades of seconds, i.e. for 120 h (cf. Fig. 8 of Ref. [3]). On the very crystal surface, perpendicular to the surface, in the absence of facets, there is a radial chemical potential difference per atom (i.e. by definition, the local absolute supersaturation) responsible for the local growth of the surface. The gradient of this supersaturation is the driving force for growth. The rate of the growth is a function of supersaturation. The supersaturation is inversely proportional to the crystal radius. For example, for one of our crystals [3], the imposed growth rate has decreased continuously from, say, 60 nm/s at the moment when crystal starts growing around the capillary tip to less than 4 nm/s when crystal radius reaches 1 mm.

The surfaces of our spherical crystals during growth have comprised both rough, rounded parts and atomically smooth facets (cf. Fig. 3 and Ref. [3]). In the presence of the supersaturation, the rough parts grow continuously, while the facets, if free of dislocations, may advance only upon penetration of the threshold for the 2D nucleation process which causes the sudden multilayer growth [5,6]. During the intervals in which the facet resists to grow vertically, it pronouncedly grows laterally [5]. In spite of the fact that in our experiments the gradient of the chemical potential on the crystal surface driving the growth has been decreasing continuously during growth, we observe the similarity of the growth mode of our crystals with the growth features detected during the growth of ^{4}He crystals under the conditions of constant chemical potential. Namely, we observe the alternation of time intervals during which the facet grows with the ones with the growth absent [5,7], i.e. the growth resembling, by occurrence of these alternating time intervals, the burst-like growth mode, as originally described in Refs. [1,2]. We note that the term "burst" is not appropriate to describe the behaviour of facets during our growth, since it involves the avalanche facet growth, as described in connection with ^{4}He crystals growth [1,2], while in our case we are dealing only with enhanced, above the average, facet vertical growth. We stress that the existence of such growing mode is the characteristic of the growth of exclusively dislocation-free facets [1,2].

In this paper, we would like to test whether the existence of facets (in our case $\{1\,1\,1\}$), free of dislocations, when formed on the surface of growing spherical crystal, may cause the accumulation of copper atoms establishing the local gradient of the chemical potential large enough to cause the penetration of the nucleation barrier threshold. The probability of nucleation barrier penetration is determined [8] by the factor:

$$\exp\left(-\frac{E_B}{k_B T}\right) \approx \exp\left(-\frac{d_{111}(\beta/d_{111})^2}{k_B T\,\Delta\mu_{surf}}\right), \quad (1)$$

where β is the step formation energy per unit step length, $\Delta\mu_{surf}$ is the chemical potential difference per unit volume across the facet on the growing crystal surface, and d_{111} is the separation of crystal planes in $\langle 1\,1\,1\rangle$ direction.

The above-described growth mode, in which the time intervals during which the facet grows vertically alternate with the ones during which the facet resists the growth, occurring at 800 K clearly requires the reconsideration of the model of thermal 2D nucleation as a basic mechanism of facet growth [8,9].

On the basis of the properties of crystals of superionic conductors characterized by very high Cu atoms diffusivity [4], we are going to, starting from diffusion equation for Cu atoms, write down the model stationary equation, describing, with appropriate boundary conditions, the distribution of Cu atoms in the absence of facets, as well as when the facets are present. Namely, during the growth, the crystal surface, due to the anisotropy of the surface shapes (facets and vicinal surfaces), must exhibit anisotropy in Cu atom density distribution underneath the growing surface.

The plan of the article is as follows. We first write down our model equations for calculation of copper atom density and flow distributions. We then solve these equations with boundary conditions appropriate for facet-free growth and for growth with facet present. Finally, we present and discuss these solutions. The article ends with our conclusions.

2. The model

The geometry of our model is shown in Fig. 2. The region of our modelling is a spherical segment of polar width 2θ, bounded by spheres of radii R_0 and R. The

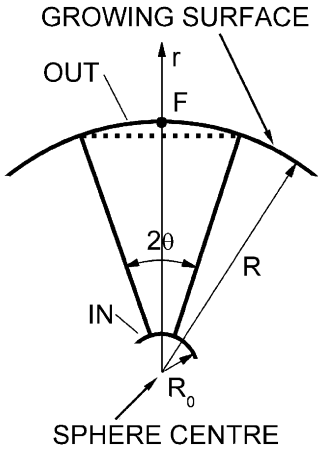

Fig. 2. Geometry of the model.

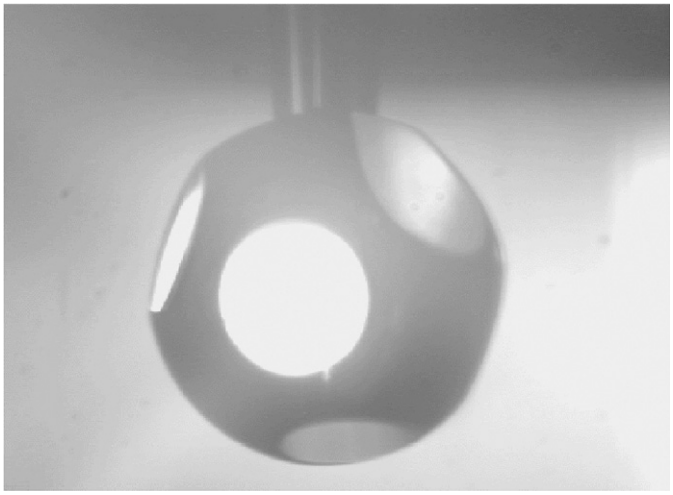

Fig. 3. Spherical copper selenide crystal during growth, featuring {1 1 1} facets, as bright circular objects on surface, and rounded parts between them (taken from Ref. [3]).

segment of the smaller sphere mimics the part of the initial hemispherical shape of the crystal upon leaving the capillary orifice (cf. Fig. 1 and Ref. [3]) and represents the source of initially radial (at R_0) flux of metallic atoms, while the corresponding segment of the outer sphere represents the part of the surface of the growing crystal. Due to the azimuthal symmetry of the problem, the azimuthal angle φ does not appear in our equations and will be henceforth suppressed, and we refer to the remaining two coordinates, r and ϑ, as radial and off-radial coordinate, respectively. This is, of course, an approximation. Namely, from Fig. 3, in which we show the shape and surface of one of our growing crystals exhibiting both {1 1 1} facets and rough parts in $\langle 1\,0\,0\rangle$ directions, in accordance with the appropriate crystal symmetry group, it is clear that a more realistic model should take into account the azimuthal anisotropy of the problem as well. Also, we have not taken into account the changes in the curvature of the rough, rounded parts of the surface [10], which is related to the lateral facet extension. These changes probably influence the total atom flux, since the effective growing area changes, but this would not have significant impact on our conclusions.

Under the stationary conditions, and for constant temperature, the density of metal atoms flow is given by [11]:

$$\vec{j}(r,\vartheta) = -D\vec{\nabla}N(r,\vartheta), \tag{2}$$

where D is the ambipolar diffusion coefficient [3]. D is isotropic since it has been shown that the net of the tunnels of the $\langle 2\,2\,0\rangle$ type, alternating between octahedral and tetrahedral sites, responsible for Cu atoms transport, is isotropic [12]. It should be noted that D depends weakly on copper ion density [3], but since only about 1% of the total copper ion density difference occurs within our volume of interest, between the centre of the spherical crystal and its surface we approximate it by a constant, $D \approx D(Cu_{1.8}Se)$ [3]. N is the Cu atoms density. Upon insertion of this equation into the continuity equation,

$$\frac{\partial N(r,\vartheta)}{\partial t} + \vec{\nabla}\vec{j}(r,\vartheta) = 0, \tag{3}$$

and by limiting ourselves to stationary conditions, we obtain the differential equation which describes the distribution of the particle density within our volume of interest:

$$\begin{aligned} &\nabla^2 N(r,\vartheta) = 0,\\ &j_r(r,\vartheta) = -D\frac{\partial N(r,\vartheta)}{\partial r},\\ &j_\vartheta(r,\vartheta) = -\frac{D}{r}\frac{\partial N(r,\vartheta)}{\partial \vartheta}. \end{aligned} \tag{4}$$

We solve this equation within the spherical segment defined in Fig. 2 for two different sets of boundary conditions. In order to simulate the facet-free growth of crystal, our boundary conditions should guarantee the radial flow of particles with fixed total incoming (at $r = R_0$) and outgoing (at $r = R$) flux of particles, $I_0^* = (I_0/2)\sin^2(\theta/2)$, with I_0 being the total flux of particles emerging from the inner sphere:

$$\int_{IN} j_r(R_0,\vartheta)\,dS = \int_G j_r(R,\vartheta)\,dS = I_0^*, \quad j_\vartheta(r,\vartheta) = 0, \tag{5}$$

where indices IN and G stand for inner sphere and growing surface, respectively.

The other case is the one in which a facet appears at the growing end of the crystal, i.e. at $r = R$. In a real situation, a facet would be formed at $r < R$. We approximate the situation by placing the facet at $r = R$ because it is more convenient for calculations. This approximation is justified by the fact that all our calculated copper ion density and chemical potential distributions (cf. Figs. 4 and 7) vary very slowly in the vicinity of $r = R$. The particles are thus forbidden to flow through the facet and are forced to leave the volume of interest through the side areas S of the spherical segment. This case corresponds to the boundary

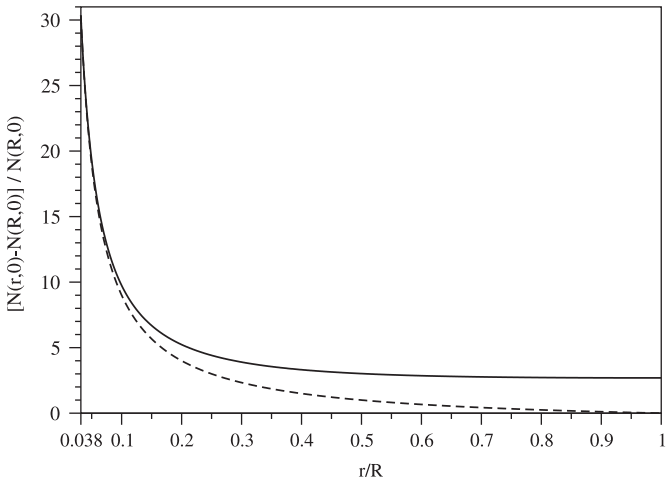

Fig. 4. Normalized density of Cu atoms along the axis pointing to the centre of the facet (for size corresponding to $\theta = 20^\circ$). Dashed line: facet-free case, full line: facet present. Both curves normalized to the incoming flux I_0^*.

conditions:

$$\int_{\mathrm{IN}} j_r(R_0,\vartheta)\,\mathrm{d}S = \int_{\mathrm{S}} j_\vartheta(r,\theta)\,\mathrm{d}S = I_0^*,$$
$$j_r(R,\vartheta) = 0, \quad j_\vartheta(R_0,\vartheta) = 0. \tag{6}$$

The solutions to Eq. (4) are as follows. For the facet-free growth case (boundary conditions (5)) the solution reads:

$$N(r,\vartheta) = \frac{I_0^*}{Dr},$$
$$j_r(r,\vartheta) = \frac{I_0^*}{r^2}. \tag{7}$$

In the case of the facet formed at the growing end of the crystal, the solution, pertinent to boundary conditions (6), reads:

$$N^{\mathrm{F}}(r,\vartheta) = N_0^{\mathrm{F}} - A\left(r^\nu + \frac{\nu}{\nu+1}R^{2\nu+1}r^{-\nu-1}\right)P_\nu(\cos\vartheta),$$
$$j_r^{\mathrm{F}}(r,\vartheta) = DA\nu\left(r^{\nu-1} - R^{2\nu+1}r^{-\nu-2}\right)P_\nu(\cos\vartheta),$$
$$j_\vartheta^{\mathrm{F}}(r,\vartheta) = DA\left(r^{\nu-1} + \frac{\nu}{\nu+1}R^{2\nu+1}r^{-\nu-2}\right) \times(-\sin\vartheta)\frac{\mathrm{d}P_\nu(\cos\vartheta)}{\mathrm{d}\vartheta}. \tag{8}$$

Here, superscript "F" denotes the case with facet present. $N_0^{\mathrm{F}} = N^{\mathrm{F}}(R_0,0)$, A is a constant determined by the first boundary condition (6), and ν is a real constant determined through boundary conditions by

$$-\frac{\nu}{\nu+1} = \left(\frac{R_0}{R}\right)^{2\nu+1}. \tag{9}$$

$P_\nu(\cos\vartheta)$ denotes the Legendre polynomial of the first kind.

3. Results and discussion

For the quantities $\Delta\mu = \mu_0 - \mu_{\mathrm{G}}$ (chemical potential difference between the site of injection of metallic atoms and the growing end of the crystal) and the radii of inner and outer spheres bordering our spherical segment of interest, R_0 and R, respectively, we have chosen the typical values from our experiments, $\Delta\mu = 0.5\,\mathrm{eV}$, $R = 1\,\mathrm{mm}$, and $R_0 = 0.038\,\mathrm{mm}$ (cf. Table 1 in Ref. [3]). We note that throughout this paper by chemical potential we mean chemical potential per copper atom unless explicitly stated otherwise. Since the major part (more than 98%) of the difference of the chemical potential occurs between the injection site of the metal atoms and the hemispherical shape formed upon the growth of crystal just outside of the capillary orifice [3] (corresponding to the small inner sphere in our model), we have in our calculation adopted the value

$$\mu_{\mathrm{IN}} - \mu_{\mathrm{G}} = 10\,(\mathrm{meV}) \tag{10}$$

for the chemical potential difference (per copper atom) between the inner sphere (IN) and growing end (G) of the crystal. The chosen values of R_0 and R define, by means of Eq. (9), the value of the exponent ν in Eqs. (8) to be $\nu = -0.95$.

In Fig. 4, we plot the calculated values of the metal atoms densities as functions of reduced radial coordinate r/R along the symmetry axis of the spherical segment ($\vartheta = 0^0$) for the facet-free case (dashed line) and for the case with facet present (full line). While in the former case the density of copper atoms decreases inversely proportional with r, in the latter case the particles accumulate towards the facet increasing the chemical potential gradient, i.e. the local supersaturation (which is proportional to this gradient) which might be capable of nucleation barrier penetration. In Fig. 5, we plot the corresponding densities of metal atoms flow. Fig. 5a depicts its radial component along the symmetry axis for facet-free case (dashed line) and in case with facet present (full line). In the latter case, the density of metal atoms flow drops to zero reflecting the fact imposed by our boundary condition that the particles cannot penetrate through the facet. In Fig. 5b we plot the off-radial component of the density of metal atoms flow, which, for $R_0 < r \leqslant R$, describes the transport of particles outwards of the spherical segment through its side area. We plot it along the inner side of the facet, i.e. $j_\vartheta^{\mathrm{F}}(r = R,\vartheta)$. This density depends on the facet size, determined by the size of the angle θ, which has been taken to be 20° in Fig. 5b, corresponding to the facet "radius" (in our model half-facet arch) of $0.35R$. We have chosen the quantity $\tan\theta$ as a measure of our model facet size, since $\tan\theta$ is the ratio of facet radius to its separation from the sphere centre, and, consequently, for the situation when the facet does not grow vertically, it directly measures the facet radius, i.e. its size.

By means of these metal atoms flow densities, we calculate the corresponding chemical potential differences. In the facet-free case, the total difference of chemical

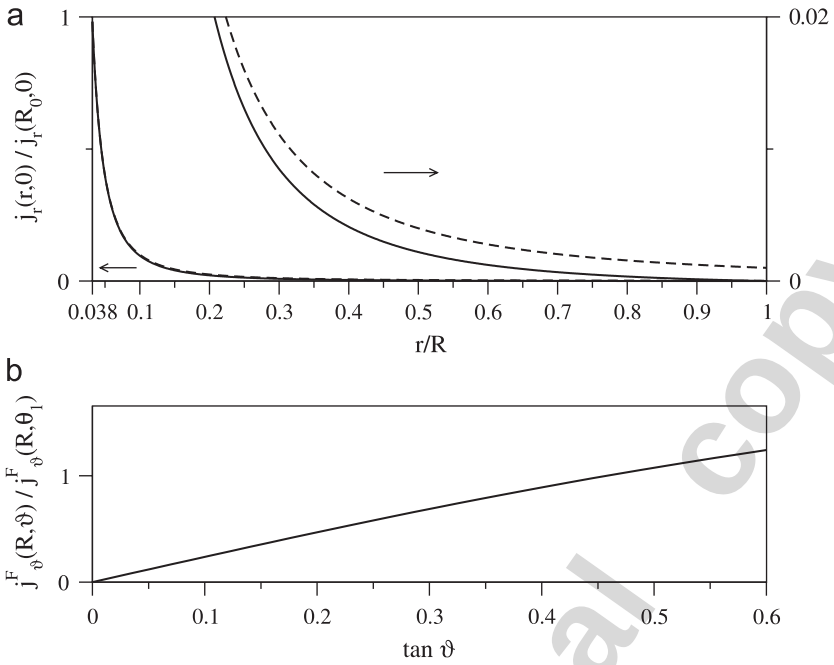

Fig. 5. (a) Normalized radial component of the density of Cu atoms flux. Dashed line: facet-free case, full line: facet present ($\theta = 20^\circ$). Both curves normalized to the incoming flux at $r = R_0$. Please note that both curves are plotted twice, the upper ones refer to ordinate on the right side, enlarged by a factor of 50. (b) Normalized off-radial component of the Cu atoms flux density on the facet, normalized with respect to $j^F(r = R, \theta_1 = 20^\circ)$, as a function of the facet size.

potential happens between the inner sphere (IN) and the growing end (G) of the crystal (G). This chemical potential difference is given by [3]:

$$\mu_{IN} - \mu_G = -\frac{e}{\sigma_i}\int_{R_0}^{R} dr\, j_r(r,\vartheta) = B\left(\frac{1}{R_0} - \frac{1}{R}\right). \quad (11)$$

Here, e is the electronic charge and σ_i is the ionic conductivity which we have approximated by a constant [3]. The constant B is determined by the estimate (10), $B = 0.395\,\text{meV mm}$. The chemical potential as a function of radial separation from the centre of the sphere is obtained as:

$$\mu(r) - \mu_G = -\frac{e}{\sigma_i}\int_{r}^{R} dr\, j_r(r,\vartheta) = B\left(\frac{1}{r} - \frac{1}{R}\right). \quad (12)$$

We plot this dependence in Fig. 6.

In the case in which a facet is present, the chemical potential balance is as follows. The total difference of chemical potential between the atom source (inner sphere) and the growing end of the crystal, i.e. the facet edge defined within our model by a circle $r = R$, $\vartheta = \theta$, is approximately given by:

$$\begin{aligned}\mu_{IN} - \mu_G &= (\mu_{IN} - \mu_F) + (\mu_F - \mu_G)\\ &= -\frac{e}{\sigma_i}\int_{R_0}^{R} dr\, j_r^F(r,0) - \frac{e}{\sigma_i} R\int_0^{\theta} d\vartheta\, j_\vartheta^F(R,\vartheta)\\ &= C\frac{2v+1}{v+1} + C\frac{2v+1}{v+1}(P_v(\cos\theta) - 1)\\ &= C\frac{2v+1}{v+1}P_v(\cos\theta). \end{aligned} \quad (13)$$

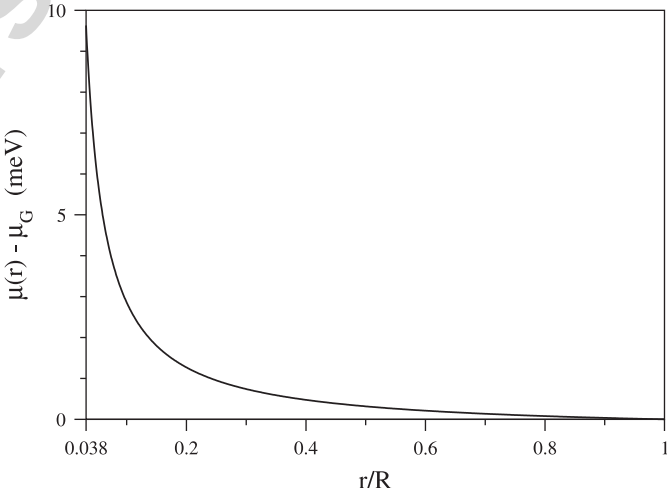

Fig. 6. Chemical potential relative to the growing end of the crystal for spherical crystal without facets. (Note that the chemical potential of the growing end is constant during the growth, fixed by Se vapour pressure.)

The superscript "F" denotes the centre of the facet (cf. point F in Fig. 2). The particle flux densities j_r^F and j_ϑ^F are given by Eq. (8), and the constant C is determined, as before, by the condition (10). The first terms on the right-hand side of first three equation lines correspond to the chemical potential difference along the symmetry axis between the inner sphere and the centre of the facet, while the second terms represent the chemical potential difference along the facet radius, i.e. between the facet centre and its edge. The chemical potential as a function of the radial

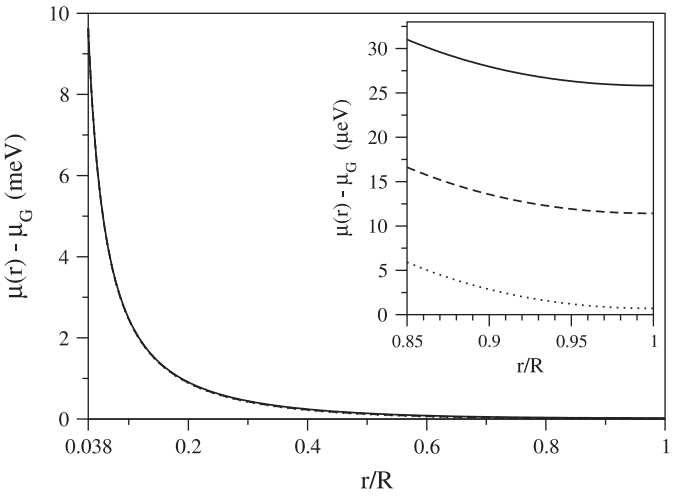

Fig. 7. Chemical potential relative to the growing end of the crystal (for the growth with facet present). Dotted line: $\theta = 5^\circ$, dashed line: $\theta = 20^\circ$, full line: $\theta = 30^\circ$. *Inset*: enlarged area near the facet.

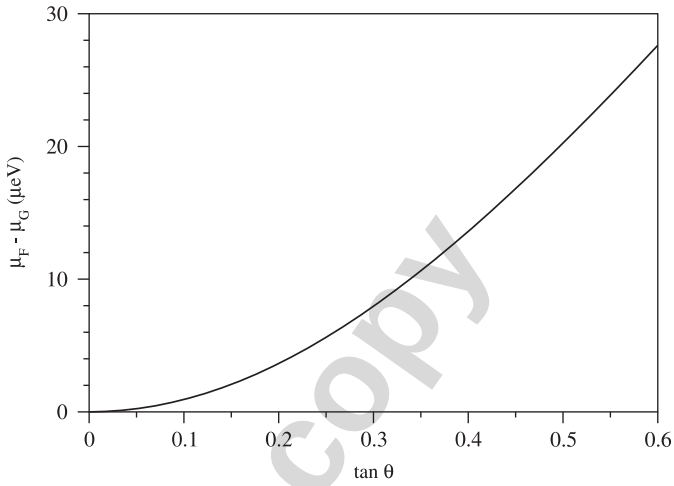

Fig. 8. Chemical potential difference between the centre of the facet and the facet edge (the position where growth takes place) as a function of facet size.

coordinate r is given by:

$$\begin{aligned}\mu(r) - \mu_G &= (\mu(r) - \mu_F) + (\mu_F - \mu_G) \\ &= -\frac{e}{\sigma_i}\int_r^R \mathrm{d}r\, j_r^F(r,0) - \frac{e}{\sigma_i} R \int_0^\theta \mathrm{d}\vartheta\, j_\vartheta^F \\ &= C\left(\frac{2v+1}{v+1} - r^v - \frac{v}{v+1} r^{-v-1}\right) \\ &\quad + C\frac{2v+1}{v+1}(P_v(\cos\theta) - 1). \end{aligned} \tag{14}$$

This dependence is plotted in Fig. 7 for various facet sizes ($\theta = 5^\circ$, 20° and 30°). The inset shows the enlarged part of this figure close to the centre of the facet. In Fig. 8, we plot the second term, i.e. the chemical potential difference between the inner and outer side of the facet, as a function of the facet size, i.e. of $\tan\theta$.

Although the difference of the chemical potential across the facet represents a small fraction of the total chemical potential difference of 10 meV (being between 0.007% and 0.26% of it for facet sizes of Fig. 7), the corresponding chemical potential differences on the very surface of the crystal, being between 0.7×10^{-3} meV (for $\theta = 5^\circ$) and 26×10^{-3} meV (for $\theta = 30^\circ$), are a few orders of magnitude larger than in the case of the facet-free growth. In the latter case, this chemical potential difference (i.e. the local absolute supersaturation) may be estimated by means of Eq. (12), being

$$w \left.\frac{\partial \mu(r)}{\partial r}\right|_{\text{surface}} \approx w \frac{B}{R^2}, \tag{15}$$

where w is the thickness of the facet, which may be taken to be at least the thickness of the molecular layer of the crystal (intermolecular distance in $\langle 1\,1\,1 \rangle$ direction), $w = a\sqrt{3}/3$, with $a = 0.5821$ nm being the dimension of the crystal unit cell. This gives for the chemical potential difference per atom a value of approximately 1.3×10^{-7} meV. It should be noted that this value agrees well with the value deduced from growth experiments [3] for the chemical potential difference per unit volume at the growing surface, being 2.6 erg/cm^3, which, upon multiplication by the unit cell volume per atom $\Omega \approx a^3/7$, gives for the chemical potential difference per copper atom the value of 4.6×10^{-8} meV. Both values are dramatically lower than the corresponding calculated values, 0.7–26×10^{-3} meV, when facet is present (cf. Fig. 7). It is important to stress that the chemical potential difference in the presence of the facet need not reach the values calculated within our model, since the chemical potential difference necessary to penetrate the nucleation barrier might establish at much lower value. We note that our calculated chemical potential difference values are significantly larger than the expected values for the formation of a facet based on our growth experiments (cf. Eq. (1) and Ref. [5]). The possible reason for this discrepancy lies in the sensitivity of our model results to the exponent v, i.e. to the inner sphere radius R_0 (cf. Eq. (9)), which in our model defines the source area of the radial incoming flow of copper atoms. As discussed in Ref. [3], the determination of R_0 is ambiguous, since it is hard to determine the moment in which the crystal acquires its (quasi)spherical shape. We have therefore chosen the value of R_0 corresponding to the inner radius of the capillary orifice. R_0 may in fact be smaller, since the growing crystal need not necessarily occupy the whole inner volume of the capillary orifice. We note that our model, for smaller values of R_0, yields significantly smaller values for the chemical potential difference at the facet, and in this case the model would yield the values that would be in good quantitative agreement with the experimental values.

4. Conclusions

We may conclude that during the growth of faceted spherical crystal, apparently without dislocations, a local chemical potential difference across the facet may be large

enough to reach the threshold value for facet growth. This will enable us to reconsider the thermal 2D nucleation as the basic mechanism of the growth mode of our copper selenide crystals at about 800 K, as detected in our preliminary growth experiments [3,5,7]. This growth, by alternation of time intervals during which facet advances vertically and the intervals during which the facet does not grow, resembles the burst-like growth mode of ^{4}He at mK temperatures [1,2]. We stress that even under the circumstances of extremely slow growth (growth rate being lower than 1 nm/s), i.e. of the extremely small average chemical potential gradient at the growing site, the facet appearance and its size changes may cause the redistribution of copper atoms density in such a way that it yields the values of the local chemical potential gradient across the facet that are much larger than the ones necessary to surmount the nucleation barrier threshold, and to initiate the vertical growth of the facet.

Acknowledgement

We gratefully acknowledge the financial support by the Ministry of Science, Education and Sport of the Republic of Croatia.

References

[1] J.P. Ruutu, P.J. Hakonen, J.S. Penttilä, A.V. Babkin, J.P. Saramäki, E.B. Sonin, Phys. Rev. Lett. 77 (1996) 2514.
[2] J.P. Ruutu, P.J. Hakonen, A.V. Babkin, A.Ya. Parshin, G. Tvalashvili, J. Low Temp. Phys. 112 (1998) 117.
[3] Z. Vučić, J. Gladić, J. Crystal Growth 205 (1999) 136.
[4] M. Horvatić, I. Aviani, M. Ilić, Solid State Ionics 34 (1989) 21;
M. Horvatić, Z. Vučić, Solid State Ionics 13 (1984) 117;
M. Horvatić, Z. Vučić, J. Gladić, M. Ilić, I. Aviani, Solid State Ionics 27 (1988) 31.
[5] Z. Vučić, J. Gladić, Fizika A 9 (2000) 9.
[6] D. Lovrić, Z. Vučić, J. Gladić, to be published.
[7] Z. Vučić, J. Gladić, D. Lovrić, S. Mitrović, M. Milas, N. Demoli, Third Scientific Meeting of the Croatian Physical Society, Book of Abstracts, 2001, p. 113;
D. Lovrić, Z. Vučić, J. Gladić, N. Demoli, S. Mitrović, M. Milas, Appl. Opt. 42 (2003) 1477.
[8] A.A. Chernov, Modern Crystallography III (Crystal Growth), Springer, Berlin-Heidelberg-New York-Tokyo, 1984 (Chapters 2 and 3).
[9] P.E. Wolf, F. Gallet, S. Balibar, E. Rolley, P. Nozières, J. Phys. 46 (1985) 1987.
[10] J. Gladić, Z. Vučić, D. Lovrić, J. Crystal Growth 242 (2002) 517.
[11] T. Ohachi, S. Imai, T. Tanaka, H. Yamai, I. Taniguchi, Solid State Ionics 28–30 (1988) 1160;
I. Yokota, J. Phys. Soc. Japan 16 (1961) 2213.
[12] M. Oliveria, R.K. McMullan, B.J. Wuensch, Solid State Ionics 28–30 (1988) 1332.